eChem
https://www.sciltp.com/journals/eChem

Review

Synergistic Catalysis in Electrocatalytic Nitrate Reduction

Jinzhi Lu †, Hao Wang †, Yongying Mou and Yan Zhu *

State Key Laboratory of Coordination Chemistry, Key Laboratory of Mesoscopic Chemistry of Ministry of Education, School of Chemistry and Chemical Engineering, Nanjing University, Nanjing 210023, China
* Correspondence: zhuyan@nju.edu.cn
† These authors contributed equally to this work.

How To Cite: Lu, J.; Wang, H.; Mou, Y.; et al. Synergistic Catalysis in Electrocatalytic Nitrate Reduction. *eChem* **2026**, *2*(1), 4. https://doi.org/10.53941/echem.2026.100004

Received: 16 April 2026
Revised: 18 May 2026
Accepted: 8 June 2026
Published: 18 June 2026

Abstract: Synergistic catalysis, through cooperative effects between two active sites or among multiple active sites, can efficiently drive multi-step complex reactions, and bifunctional or multifunctional active sites have been established on homogeneous and heterogeneous catalysts. A profound understanding of the synergistic mechanisms of these catalysts is crucial for achieving rational catalyst design and high-performance regulation. Accordingly, the article highlights the application of increasing scales of metal active sites (single-atom catalysts, dual-atom catalysts, metal clusters, and nanoparticles) in the electrocatalytic nitrate reduction reaction, given that this reaction involves a complex network featuring multiple proton-electron transfer steps and a variety of reaction intermediates. Finally, future design directions for synergistic catalysts are envisaged, aiming to provide insights for developing highly efficient ammonia synthesis catalysts and theoretical references for elucidating the essence of synergistic catalysis.

Keywords: synergistic catalysis; ammonia production; rational design; multi-site cooperation

1. Introduction

Catalytic science and technology have already played a significant role in fields such as chemical engineering, energy, and the environment, and will continue serving as a key technological pathway to address critical challenges for sustainable social development, such as resource scarcity and environmental protection. Generally, catalytic reactions are not linear processes that proceed directly from a single reactant to the final product, but rather involve complex pathways such as multi-step cascades or competitive parallel routes [1,2]. For instance, the hydroformylation reaction typically proceeds through a series of elementary steps, including H_2 activation, CO insertion and olefin insertion, with the latter determining the product's regioselectivity [3]. Consequently, in complex reaction systems, the multi-site synergistic effects of catalysts play a critical role in enhancing both reactivity and selectivity [4]. By carefully designing synergistic interactions among active sites, interfaces, or compositional elements in a catalyst, it is possible to achieve highly efficient activation of reactant molecules, stable transfer of key intermediates, and selective formation of target products. The resulting catalytic efficiency often far exceeds the individual contribution of each component [5]. For example, Christ et al. developed an atomically dispersed Rh-WO_x pair-site catalyst for efficient hydroformylation, exhibiting > 95% selectivity toward propanal with a formation rate of 0.1 g cm^{-3} h^{-1}. Based on a precisely constructed Rh-WO_x interface, this catalyst enabled a unique synergistic mechanism: CO adsorbed at Rh sites, ethylene adsorbed preferentially on WO_x before migrating to Rh, and H_2 underwent heterolytic cleavage at the Rh-WO_x interface [6]. For another example, the electrochemical CO_2 reduction reaction constitutes a multi-electron-proton transfer process involving complex intermediates and facing intense competition from the hydrogen evolution reaction (HER), resulting in low CO_2 conversion efficiency and poor product selectivity [7]. To address this issue, a dual-atom (Ni/Cu-N-C) catalyst was developed, in which the covalently bonded Cu modulated the 3d orbital configuration of Ni, thereby accelerating the adsorption process of *COOH and reducing the

dissociation kinetics of water molecules, achieving a remarkable turnover frequency of 20,695 h^{-1} and an outstanding CO Faradaic Efficiency (FE) of 97.7%, significantly outperforming its single-atom counterparts [8]. Beyond this, Figure 1 shows that synergistic catalysis has been successfully applied to a series of reactions [8–16]. These successful cases collectively reveal a core principle: through the systematic coupling of multiple components and mechanisms, synergistic catalysis can effectively overcome the limitations of isolated active sites when confronting multi-step, multi-electron transfer reactions.

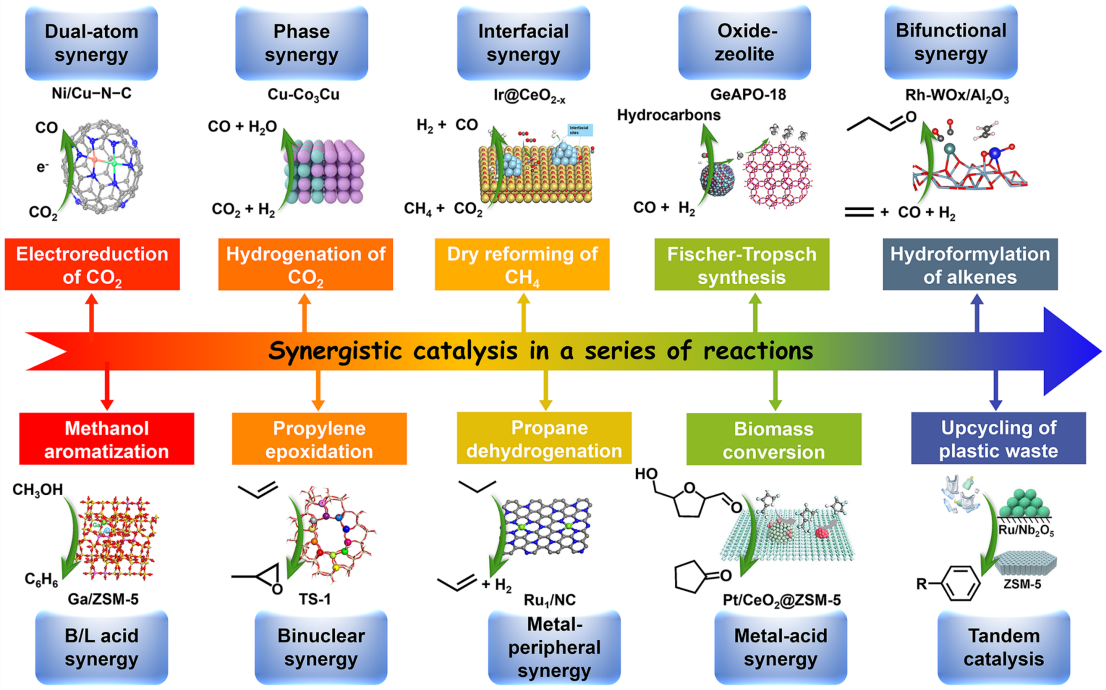

Figure 1. Significant advances in synergistic catalysis for a series of reactions.

The electrochemical reduction of nitrate to ammonia (NO_3RR) is a typical multi-proton-electron transfer reaction involving multiple intermediates, which inevitably renders the reaction process complex [17–19]. Crucially, the selective conversion of nitrate pollutants, which are widely present in wastewater, into high-value-added ammonia achieves the dual advantages of environmental remediation and resource recovery [20]. In this review, we aim to discuss the current state of research on synergistic catalysts for NO_3RR, with a particular focus on design strategies for such catalysts, covering single-atom catalysts (SACs), dual-atom catalysts (DACs), metal cluster catalysts, and metal nanoparticle catalysts. On the basis of this overview, we delve into the reaction mechanisms of synergistic catalysis and outline the future challenges and development directions in this field, providing guidance for designing the next generation of highly efficient and stable NO_3RR catalysts.

2. Design Strategies for Synergistic Catalysts

Synergistic catalysis describes a process in which two or more catalytic sites cooperate via direct or indirect interactions to promote the chemical transformation, achieving a catalytic effect that surpasses the sum of individual contributions [21]. Multi-site synergistic catalysis, as a reliable solution for enhancing the activity, selectivity, and stability of catalysts, especially those involving multiple elementary steps, has been well-established through extensive research over the past decades. Although these studies cover different metal scales (atoms [22,23], clusters [24] and nanoparticles [25]), different catalytic modalities (homogeneous catalysis [1], heterogeneous catalysis [26], photocatalysis [27], electrocatalysis [28]) and different substrate materials (metals [29], metal oxides [30], organic-inorganic hybrid materials [31], et al.), they still adhere to the same, fundamental catalyst design strategies. Herein, the strategies are summarized into three aspects: adjacency in space, interdependency in structure, and cooperation in function (Figure 2).

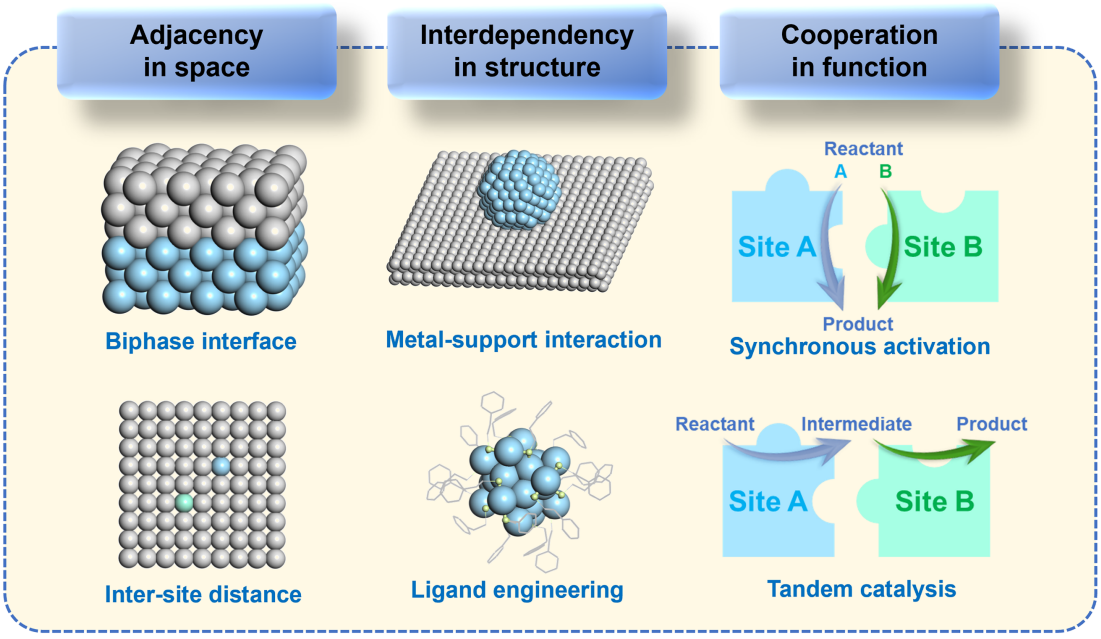

Figure 2. Typical design concepts for synergistic catalysts.

2.1. Adjacency in Space

The diameter of the substrate molecules in catalytic reactions are usually several angstroms, which determines that the spatial distance between the synergistic catalytic sites is typically at a similar scale [32]. For multi-component catalysts, contact at such scale occurs at the interfaces of each component, such as metal-metal interface [33], metal-metal oxide interfaces [34], heterojunctions [35], etc.

For supported catalysts, enhancing the dispersion of the metal on the support is the most straightforward way to increase the number of interface cooperative sites. Single-atom catalysts (SACs) maximize the dispersion of the metal, ensuring that each metal atom participates in the construction of interface cooperative sites, thereby achieving high catalytic performance and atomic utilization [36–38]. Modifying the combination of components, such as core-shell structures and sandwich structures [39–41], can also enhance and stabilize the interface cooperative sites. Furthermore, spatially adjacent cooperative catalytic sites can also be constructed through methods such as doping and alloying [42,43].

Furthermore, with the advancement of catalyst preparation technology, it has been possible to control the distances between different catalytic sites. Typically, the spacing between single atom and single atom, single atom and cluster, or single atom and nanoparticle has become a controllable factor in regulating catalytic performance, broadening the design strategies for synergistic catalysts [44–46]. Based on this, the concept of inter-site distance (ISD) has been introduced, providing a quantitative basis for the spatial proximity principle in synergistic catalyst design [47].

2.2. Interdependency in Structure

In a complex multi-component synergistic catalytic system, the various components are usually not independent. Instead, they serve as prerequisites for each other's unique structure while simultaneously interacting with one another. Such interaction includes charge transfer, coordinated mode regulation, formation of special interface sites, and so on.

Typically, for supported catalysts, the interdependency of metal nanoparticles and supports was concluded as the metal-support interaction (MSI), which has been studied deeply and applied widely in catalytic research [48–50]. The carrier stabilizes specific-sized metal particles, preventing their sintering and deactivation. Driven by differences in the Fermi level of the metal nanoparticles and the supports, charge transfer often occurs at the interface of them, leading to a rearrangement of electrons within both materials [51]. What's more, the metals and supports jointly form special interface structures due to the intense interactions, such as interface defect sites, partially covered layers and so on.

At the atomically precise structural level, the interdependence between metal atoms and the coordination environment is also a prerequisite for establishing cooperative catalytic effects. For single-atom catalysts, an individual metal site must rely on the surrounding coordination environment to exist, such as C, N, S, or P [52–55].

Together, they constitute the so-called single-atom active sites in which both components are indispensable. Ligand-protected, atomically precise metal nanoclusters are representative examples of the interdependence between the metal core and ligands. The type and coordination modes of peripheral ligands are essential for maintaining the atomic-precise structure of clusters. Together, the metal core and ligands form a molecule-like sub-nanometric structure, which exhibits drastically different catalytic properties compared to ligand-free metal clusters or metal nanoparticles. Thus, this offers a promising avenue for the design of novel cooperative catalysts and research into their underlying mechanisms [56,57].

2.3. Cooperation in Function

After centuries of development in catalysis, the roles of various catalytic sites (such as Lewis acid, Brønsted acid, base, lattice oxygen, defect sites, etc.) in catalytic processes have become relatively well understood [58–62]. For complex reactions that require the activation of multiple substrate molecules or involve multiple elementary steps, the design of multifunctional catalysts based on existing experience of catalytic sites serves as the goal for achieving synergistic catalysis [63,64].

For reactions requiring the activation of multiple substrates, a common strategy in synergistic catalyst design is to employ distinct functional sites that can activate the corresponding molecules separately. Taking the DRM mentioned before as an example, this reaction requires the simultaneous activation of both CH_4 and CO_2. Since the CO_2 activation capability of typical metal sites (Ni, Ru, etc.) is significantly weaker than that of CH_4, carbon deposition resulting from CH_4 cracking cannot be removed in time, which has become the major bottleneck for the scalable application of DRM [65,66]. Introducing basic sites, oxygen vacancies, or similar features to enhance CO_2 activation offers a feasible approach to constructing highly stable DRM catalysts [67,68]. Similarly, many reactions following the Langmuir-Hinshelwood mechanism can achieve enhanced catalytic performance through the design of synergistic catalytic sites [24,69].

For complex reactions involving multiple steps, different catalytic sites may be necessary for different elementary steps. The construction of oxide-zeolite composite catalysts serves as a typical example of tandem cooperative catalysis. On the one hand, the regular pore structure of zeolites enables shape-selective catalysis, thereby regulating the regioselectivity of the reaction. On the other hand, small molecules are adsorbed and activated on oxide sites to form reactive intermediates, which subsequently react at the acidic centers of the zeolite to yield higher-value products. This approach offers a promising pathway for the conversion of syngas, CO_2, and similar feedstocks into a wider range of chemicals [13,70].

In summary, synergistic catalysis follows a layered logic of physical constraints, chemical origins, and functional realization. Spatial adjacency serves as the physical prerequisite for synergy, ensuring that the active sites operate within an angstrom-scale range; structural interdependence constitutes the chemical foundation of the synergistic effect, creating new activities through electronic and structural interactions. Together, they enable the ultimate achievement of functional cooperativity, completing a closed-loop progression from fundamental design to highly efficient catalysis.

3. Applications of Synergistic Catalysis in NO_3RR

Given the critical role of ammonia in both the chemical industry and agricultural production, as well as the significant advantages of the NO_3RR in environmental remediation, emerging synergistic catalytic design strategies have been widely applied in the development of NO_3RR catalysts. This section focuses on the application of synergistic catalytic strategies in NO_3RR, with particular emphasis on the scale of metal active sites. From the perspective of the atomic scale of metals, the construction of single-atom, dual-atom, and cluster catalysts is systematically discussed. On this basis, metal cluster catalysts are further categorized into organic ligand-protected and ligand-free systems. In addition, a brief discussion is also provided on synergistic catalysis at the scale of metal nanoparticles. For SACs, the synergy is predominantly structural interdependence between the metal centers and the support, which enhances catalytic performance by modulating the coordination environment and electronic structure of the active sites. In contrast, the most distinctive feature of DACs is the spatial adjacency synergy between the two metal atoms, which effectively promotes substrate adsorption and lowers the energy barrier of key reaction steps. Furthermore, for metal cluster and metal nanoparticle catalysts, the primary synergy arises from the structural interdependence among adjacent metal atoms either within the clusters or between nanoparticles. Notably, although the above catalysts differ in their structural design strategies, they are often accompanied by functional cooperation during catalytic processes. That is, the various catalytic centers collaborate and divide labor in different steps, such as reactant activation, intermediate stabilization, and product release, thereby collectively enhancing catalytic activity, selectivity, and stability.

3.1. Single-Atom Catalyst

For SACs, we have primarily elucidated the synergy of structural interdependence between the metal center and its local coordination environment. Specifically, metal atoms give rise to highly tunable catalytic active sites through electronic interactions and geometric configuration matching with surrounding coordinating atoms (such as S, N, and O).

Interface manipulation at the atomic level to regulate the environment of active sites, such as electronic structure and coordination environment, holds significant importance for the design and construction of advanced SACs [36,71]. The NO_3RR involves complex multi-electron-proton coupled transfer processes, during which various intermediate species (such as NO_2^-, NO, NH_2OH) may be generated. Consequently, achieving efficient and highly selective reduction of NO_3^- to NH_3 on catalysts with only a single site is often challenging. To overcome this limitation, recent research has focused on maintaining the structural uniformity and high intrinsic activity of SACs while further optimizing mass transport of reactants, adsorption/desorption behaviors of intermediates, and electronic structures of catalysts through strategies such as introducing supports with ordered porous structures or doping with non-metallic elements, thereby enhancing catalytic performance. For instance, Wei et al. developed an in situ anisotropic etching-induced strategy using MOFs as precursors to successfully synthesize a two-dimensional monolayer hierarchical porous honeycomb-like carbon catalyst embedded with Co-N_4S_1 sites (Figure 3a) [72]. This catalyst exhibited an outstanding performance in the NO_3RR, achieving an NH_3 FE of 88.78% and an NH_3 production rate of 9.46 mg h^{-1} mg_{cat}^{-1}. Mechanistic studies revealed that the unique coordination structure of the cobalt sites in Co-N_4S_1 shifted the d-band center toward the Fermi level, thereby lowering the reaction barrier of the rate-determining step (*NOH → *N) and enhancing the adsorption of the *N intermediates (Figure 3b,c). Furthermore, the distinctive hierarchical porous honeycomb architecture significantly improved mass transport within the reaction system. This synergistic catalyst design strategy not only enabled precise modulation of the coordination environment of the active centers but also brought improvement in catalytic performance. In addition to S coordination, researchers have also explored the substitution of partial N atoms with O atoms to break the symmetry of the metal-center coordination and enhance site polarity. For example, Cheng et al. successfully prepared a Cu-based catalyst with cis-configuration coordination (Cu-cis-N_2O_2) by pyrolyzing a Cu-based polymer precursor, in which each Cu atom was coordinated in a cis manner with two N atoms and two O atoms, achieving effective regulation of coordination symmetry. Studies have shown that such symmetry breaking can significantly enhance the polarity of the active sites, thereby promoting the enrichment and activation of NO_3^- on the catalyst surface. Under an industrial-level current density as high as 366 mA cm^{-2}, the catalyst achieved an NH_3 production rate of 27.84 mg h^{-1} cm^{-2} and exhibited excellent electrochemical stability. Further mechanistic analysis revealed that the cis-coordination structure induced splitting of the Cu 3d orbital energy levels, enabling the formation of a π-complex with orbital symmetry matching that of the key reaction intermediate *ONH. Compared to the σ-complex commonly formed on conventional catalysts, this π-complex structure significantly reduced the reaction energy barrier and enhanced intrinsic activity (Figure 3d–g) [73]. This strategy of tuning coordination symmetry to synergistically optimize site polarity and electronic structure provided a novel approach for overcoming the performance limitations associated with single active sites in SACs. Li et al. successfully designed and synthesized a structurally distorted CuN_2O_2 active site anchored on a porous carbon support, denoted as Cu_{SA}-NO/C. This active center formed a complex coordination configuration with two adjacent N-doped atoms and two O-doped atoms in the support, achieving an FE of 92.7% for NH_3 and an NH_3 production rate of 24.9 mg h^{-1} mg_{Cu}^{-1} in the NO_3RR. Experimental analysis and mechanistic characterization revealed that the optimized charge transfer between adjacent O atoms and the Cu active center distributed on the porous carbon carrier significantly promoted H_2O dissociation to generate protons and effectively reduced the overall energy barrier of the reaction (Figure 3h) [74]. This study further demonstrated the important role of structural distortion in modulating the local electronic structure and geometric configuration of the central metal in M-N_4/C-type catalysts.

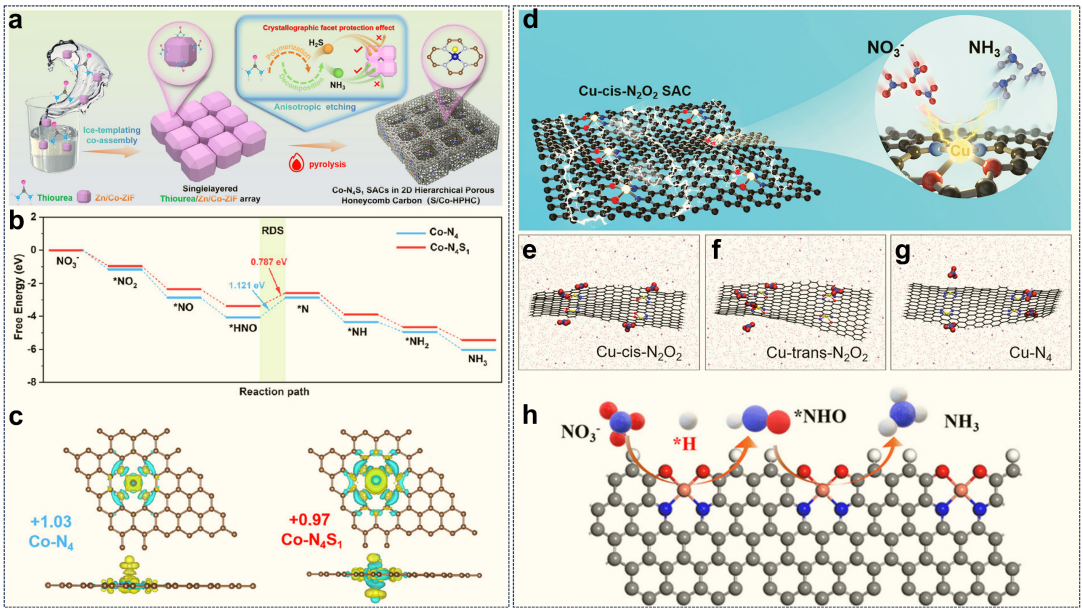

Figure 3. (**a**) The synthesis process of Co-N_4S_1 SACs catalysts, and (**b**) the Gibbs free energy diagram of Co-N_4S_1 SACs catalysts toward NO_3RR, (**c**) Bader charge analysis of the intermediates on the active sites for Co 3d orbitals and charge density differential. Reproduced with permission [72]. Copyright 2025, Wiley. (**d**) Schematic diagram of the Cu-cis-N_2O_2 SAC. Molecular dynamics simulations of (**e**) Cu-cis-N_2O_2, (**f**) Cu-trans- N_2O_2, and (**g**) Cu-N_4 SACs. Reproduced with permission [73]. Copyright 2022, Wiley. (**h**) The proposed catalytic mechanism of Cu_{SA}-NO/C toward NO_3RR. Reproduced with permission [74]. Copyright 2025, Wiley.

In brief, the synergistic effect between SACs and their coordination environments has been extensively investigated in NO_3RR. However, despite sustained efforts, the homogeneity in metal composition and dependence on the coordination environment of SACs limited the tunability of synergistic sites. Moreover, the performance remains subject to the number of monodispersed active sites.

3.2. Dual-Atom Catalysts

In the NO_3RR, the multi-proton transfer occurring at catalytic active sites frequently causes an imbalance in the protonation extent of NO_2 and NO intermediates [75]. This process also competes with the HER, leading to markedly reduced efficiency in NH_3 production. The fundamental challenge stems from the linear scaling relationship commonly observed between the adsorption strengths of conventional active sites for different intermediates [76]. Such a correlation limits the selectivity among possible protonation pathways and hinders the steering of the reaction toward the target product NH_3. To improve catalytic performance, it is crucial to break this linear adsorption scaling and achieve differentiated control over key intermediates. A promising strategy involves harnessing synergistic effects between neighboring active sites. By constructing a dual-metal-site catalytic system with complementary functions at the atomic scale, the proton-transfer process can be cooperatively optimized with the adsorption/activation of nitrogen-containing species on one site and the modulation of proton supply or suppression of the HER side reaction on the other. This spatial and functional synergy not only promotes directed protonation of intermediates but also mitigates competition with HER, significantly enhancing the FE and production rate of NH_3 generation.

3.2.1. Homometallic Dual-Atom Catalysts

Inspired by the natural Cu-dependent nitrite reductase, Wang and colleagues developed a synergistic dual-atom Cu catalyst by anchoring Cu atoms on a polymeric carbon nitride support for the NO_3RR (Figure 4a) [77]. In this catalyst, the Cu_a sites adsorbed *NO intermediates, while the neighboring Cu_b sites facilitated H_2O dissociation to produce *H species, thus supplying active hydrogen promptly for *NO reduction (Figure 4b). This cooperative mechanism between the two distinct metal sites enhanced proton transfer kinetics, leading to a high NH_3 production rate of 467 mg h^{-1} mg_{cat}^{-1}. Furthermore, the catalyst exhibited remarkable stability, operating continuously for 360 h at 6 A with a sustained NH_3 output of 11 g per day (Figure 4c). The findings suggest that this catalyst offers promising potential for sustainable and efficient electrochemical NH_3 synthesis under conditions relevant to industrial wastewater treatment.

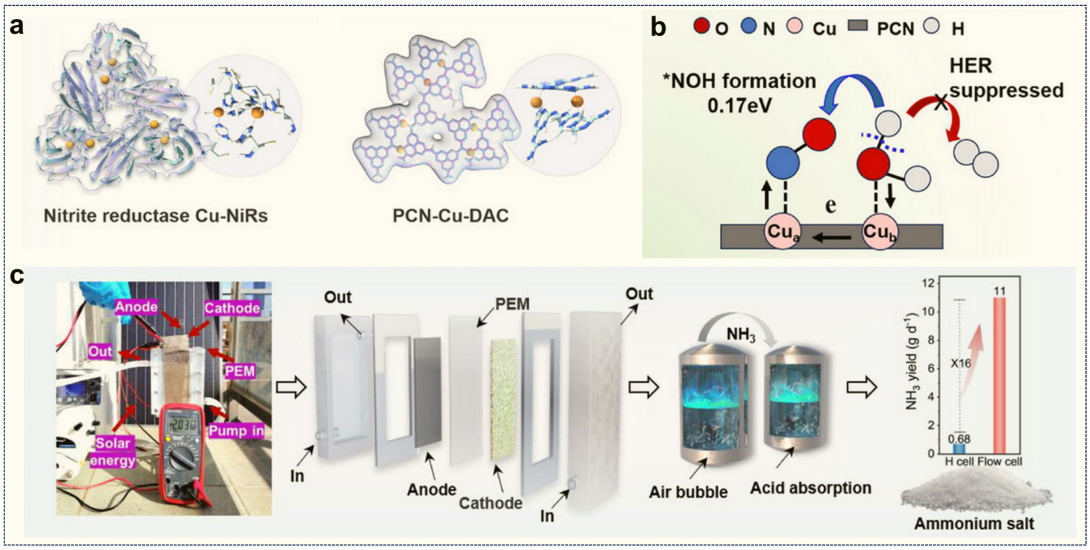

Figure 4. (**a**) Schematic diagram of the structure of native copper nitrite reductase and the diatomic copper catalyst, (**b**) mechanism of nitrate ion reduction on the surface of Cu DACs, and (**c**) schematic diagram of the flow-through cell electrocatalytic NO_3 reduction reaction. Reproduced with permission [77]. Copyright 2025, Wiley.

3.2.2. Heterometallic Dual-Atom Catalysts

Liu et al. reported a pulsed-discharge strategy for synthesizing an efficient catalyst for NO_3RR [78]. This approach involved applying microsecond pulsed currents to metal precursors supported on N-doped graphene aerogel (NGA). Through the explosive decomposition of metal salt nanocrystals, the method enabled the construction of asymmetrically coordinated diatomic sites anchored on NGA. These sites adopted a RuN_2-CuN_3 coordination configuration, denoted as RuCu DAs/NGA (Figure 5a). In NO_3RR, the catalyst achieved an FE of 95.7% and an NH_3 production rate of 3.1 mg h^{-1} cm^{-2}. It is indicated that in the well-controlled RuN_2-CuN_3 structure, the 4d orbitals of Ru are positioned closer to the Fermi level, leading to strong adsorption of reaction intermediates, while CuN_3 has a relatively weak adsorption that facilitates intermediate desorption (Figure 5b). Mechanistic investigations suggest that the asymmetrically coordinated bimetallic atoms work synergistically to catalyze the reduction of $*NO_3$ to *NO, with subsequent hydrogenation steps predominantly occurring at the Ru site (Figure 5c,d). Furthermore, this pulsed-discharge synthesis strategy exhibits good generality and can be extended to prepare various asymmetrically coordinated diatomic catalysts, such as PtCu, PdCu, FeCu, and NiCu. Efficient electrocatalytic NO_3^- reduction for NH_3 requires customized electrode engineering that integrates Cu and a second metal site uniformly at the atomic scale, overcoming interfacial heterogeneity and improving ammonia selectivity.

Currently, in addition to the aforementioned CuRu catalyst, Cu-based bimetallic materials applied in the NO_3RR also include systems such as CuCo [79] and CuNi [80] catalysts. These systems exhibit pronounced synergistic effects, wherein the bimetallic components effectively promote the reduction of NO_3^- to NH_3 through structural interdependence or functional cooperation. However, achieving high selectivity for NH_3 production at high current densities remains constrained by persistent kinetic challenges [81]. Furthermore, the spatial separation between metal atomic sites disrupts the kinetic coupling between *H supply and the reduction of nitrogen-containing intermediates [82]. However, achieving precise control over the spatial proximity of different metal atoms remains challenging due to their thermodynamic immiscibility. To address this issue, Su et al. developed an interpenetrating polymer network (IPN) to precisely regulate the spatial distribution and inter-site distance of Cu and Co active sites, enabling high selectivity for the conversion of NO_3^- to NH_3 [81]. In this network, polypyrrole (PPy) acted as a molecular bridge, binding to polystyrene sulfonate electrostatically and connecting with a poly(3,4-ethylenedioxythiophene) network via π-π stacking to form a cohesive conductive structure (Figure 5e). The atomically adjacent Cu-Co dual sites operate synergistically through a tandem catalytic mechanism: Cu sites drive the rapid reduction of NO_3^- to NO_2^-, while the neighboring Co sites supply active hydrogen species to further reduce NO_2^- to NH_3. This tandem catalytic process eliminates the kinetic bottleneck and suppresses the competing HER, achieving nearly 100% NH_3 selectivity (Figure 5f). In contrast, for the PPy-free PN-CuCo catalyst, the lack of proximal Co sites around the Cu domains suppresses the essential hydrogenation process, thereby causing the reaction to terminate prematurely at the NO_2^- intermediate. Furthermore, the IPN-CuCo DACs maintain efficient ammonia-oxygen co-production performance even at industrial-level current densities.

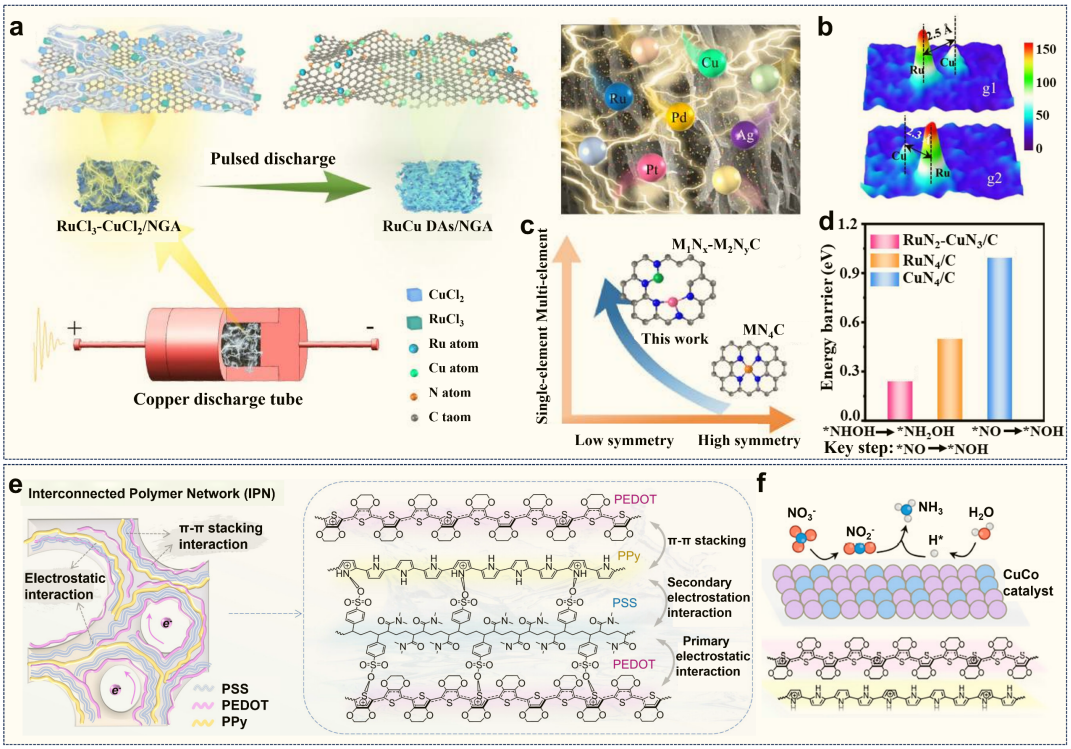

Figure 5. (**a**) The synthesis process of RuCu Das/NGA catalysts, (**b**) localized three-dimensional magnified image of RuCu DAs/NGA, (**c**) trends in asymmetric coordination structures, and (**d**) the catalytic performance for NO_3RR with different catalysts. Reproduced with permission [78]. Copyright 2025, Springer Nature. (**e**) Polymer network structure and (**f**) schematic diagram of the NO_3RR on CuCo catalysts. Reproduced with permission [81]. Copyright 2025, American Chemical Society.

Diatomic synergistic catalysis is an advanced strategy wherein two spatially adjacent, well-defined metal atoms are precisely constructed on a catalyst surface. These dual sites engage in a synergistic interplay during catalysis, optimizing reaction pathways and lowering the energy barriers of critical steps. Crucially, their close proximity facilitates the rapid transfer of reactants or intermediates, creating a unique local reaction microenvironment that dramatically enhances the efficiency and selectivity of NH_3 production.

3.3. Metal Cluster Catalysts

3.3.1. Ligand-Protected Metal Cluster Catalysts

Ligand-protected atomically precise clusters represent a special and important category of metal clusters. From a holistic level, these atomically precise clusters exhibit molecular-like electronic energy level structures and are recognized as bridging the gap between homogeneous and heterogeneous catalysts (Figure 6a) [83]. From the local level, such clusters are composed of a metal core, metal-ligand interfacial structure (e.g., staple units), and peripheral ligands (Figure 6b–d). The composition and structure of the metal core, the microstructure of the interface, and the functionality of the ligands can all be precisely regulated [84]. Furthermore, due to the precise structure and complex composition described above, the synergistic effects within clusters in catalysis become more multifaceted, including metal-ligand synergy, intermetal synergy, and cluster-support synergy.

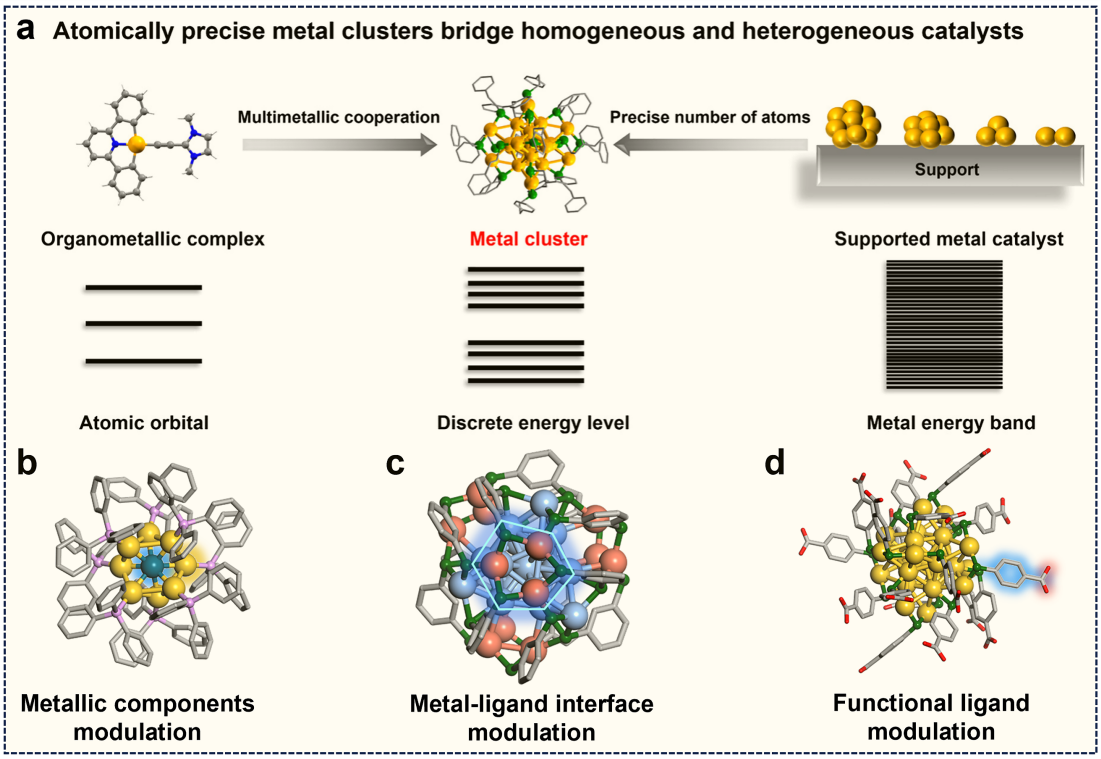

Figure 6. (**a**) Key differences among ligand-protected metal clusters, organometallic complexes, and supported metal particle catalysts. Reproduced with permission [83]. Copyright 2024, Chinese Chemical Society. Modulation of atomically precise metal clusters in their (**b**) metallic components, (**c**) metal-ligand interfaces, and (**d**) functional ligands.

For instance, Cheng et al. synthesized Cu clusters protected by different ligands for the NO_3RR, specifically $Cu_4(PTI)_4$ (PTI = $C_{12}H_3N_2OS$) and $Cu_4(BTT)_4$ (PTI = $C_{10}H_{10}NS_2$), which share the same metallic core (Figure 7a,b) [85]. Experimental results showed that strong charge interactions existed between $Cu_4(PTI)_4$ and the substrate or intermediates. This indicated that the PTI ligand, with its stronger electron-withdrawing ability, induced changes in the electronic structure of the metal active sites. Consequently, the $Cu_4(PTI)_4$ cluster achieved an FE close to 100%, significantly outperforming $Cu_4(BTT)_4$ (Figure 7c). This work demonstrated that the ligand environment can modulate the electronic structure of the metal cluster active sites, thereby tuning their catalytic performance. Qin et al. reported a bimetallic site $[Ag_{30}Pd_4(C_6H_9)_{26}](BPh_4)_2$ cluster catalyst for the NO_3RR (Figure 7d,e) [18]. The atomic precision of the ligand-protected cluster enabled precise identification of its active sites and reaction mechanism. Mechanistic investigations revealed that NO_3^- was first adsorbed onto exposed Ag sites, forming a bridged NO_3 species. This species subsequently reacted with one H_2O molecule to release NO_2^-. The NO_2^- in the electrolyte then preferentially bound to exposed Pd atoms and sequentially reacted with five H_2O molecules, ultimately yielding NH_3 (Figure 7f). With the help of this bimetallic synergistic tandem catalytic mechanism, the $[Ag_{30}Pd_4(C_6H_9)_{26}](BPh_4)_2$ cluster can get an NH_3 FE of more than 90%. Moreover, in our previous work, we successfully synthesized a bimetallic cluster comprising a single Ru atom bonded to six Au(TBBT)PPh_3 units, which was subsequently applied to the NO_3RR (Figure 7g) [86]. This catalyst successfully integrated dual-functional sites within a single Ru_1Au_6(TBBT)PPh_3 cluster catalyst, wherein the Ru site activated H_2O to yield *H. These *H subsequently migrated via an S bridge to the Au site, where they progressively reduced NO_3^- (Figure 7h). Experimental results demonstrated that the NH_3 production rate of this bimetallic cluster reached 19 times that of the Au(TBBT)PPh_3 complex. The synergistic interaction between Ru and Au within this cluster successfully achieves highly efficient NH_3 production while effectively suppressing the HER. The role of the support is also highly significant. Taking Gu et al.'s research as an example, layered double hydroxide (LDH) was used through electrostatic interactions and applied to the NO_3RR (Figure 7i) [87]. This catalyst demonstrated an NH_3 FE as high as 97%, markedly superior to the 73% achieved by pure CuFe-LDH (Figure 7j). Mechanistic studies revealed that on CuFe-LDH, the rate-determining step was NH_3 desorption; whereas in Ni_6@CuFe-LDH, the rate-determining step shifted to the reduction of $*NO_3^-$ to $*NO_2$. This work demonstrated that synergistic interactions between metal clusters and the support could effectively modulate the rate-determining step, leading to a pronounced enhancement in NH_3 generation.

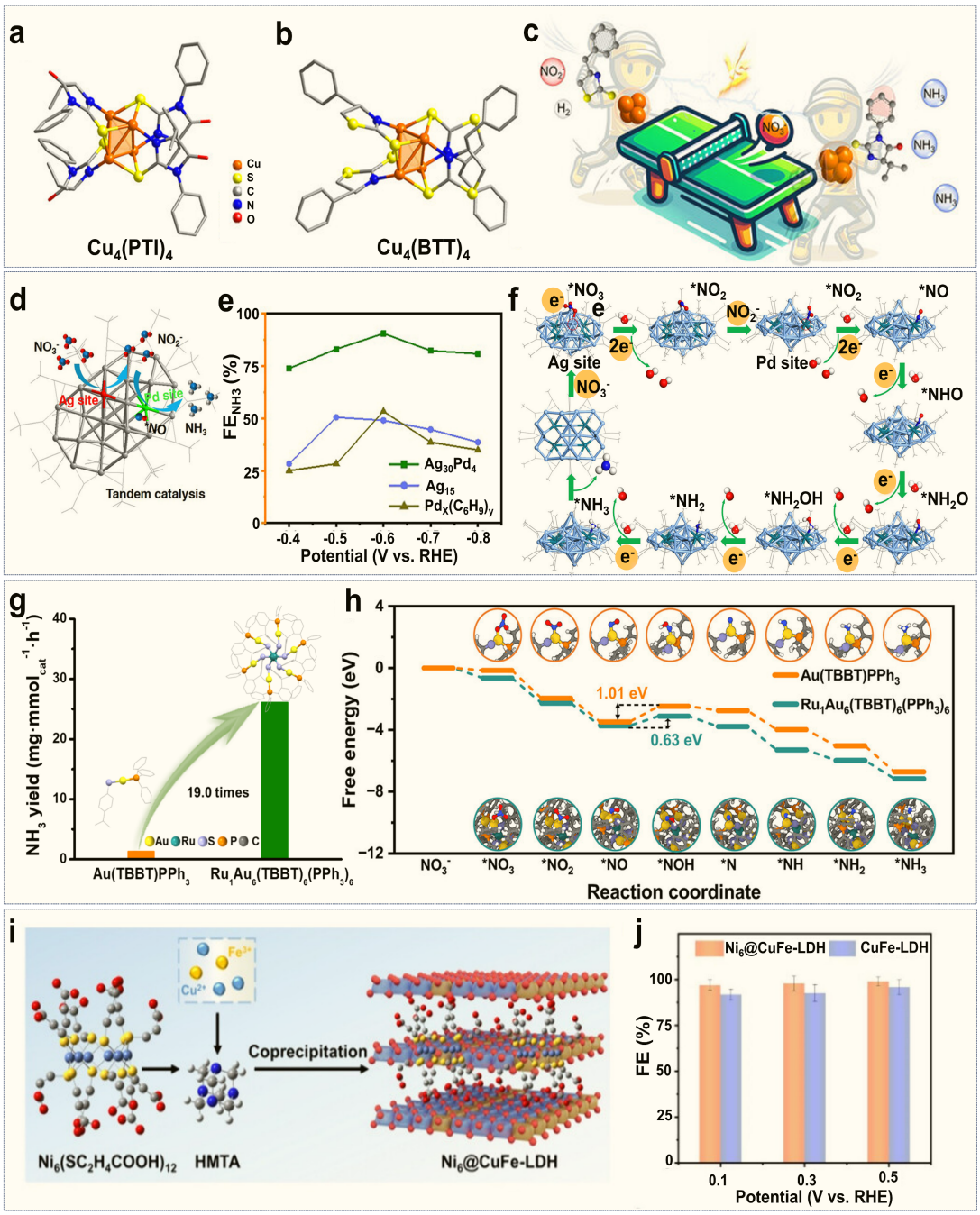

Figure 7. (**a**,**b**) The structure of $Cu_4(PTI)_4$ and $Cu_4(BTT)_4$ clusters, (**c**) schematic diagram of cluster catalysis for NO_3RR. Reproduced with permission [85]. Copyright 2025, Wiley. (**d**) The structure of $Ag_{30}Pd_4$ clusters and (**e**) its catalytic performance for NO_3RR, (**f**) reaction mechanism of NO_3RR on $Ag_{30}Pd_4$ catalysts. Reproduced with permission [18]. Copyright 2023, American Chemical Society. (**g**) The catalytic performance of $Ru_1Au_6(TBBT)_6(PPh_3)_6$ clusters for NO_3RR, and (**h**) the reaction mechanism. Reproduced with permission [86]. Copyright 2025, Wiley. (**i**) The synthesis process of Ni_6@CuFe-LDH clusters and (**j**) its catalytic performance for NO_3RR. Reproduced with permission [87]. Copyright 2025, American Chemical Society.

3.3.2. Ligand-Free Metal Cluster Catalysts

Ligand-free metal clusters feature a high density of coordination-unsaturated sites on their surfaces. This structural characteristic not only provides abundant adjacent metal active sites but also effectively modulates reaction pathways and energy barriers through interfacial synergy with the support material, resulting in significant enhancement of the electrocatalytic performance for NO_3RR. Wu et al. successfully synthesized SnCu diatomic cluster catalysts (SnCu-DG) using graphene edge defects as confinement reactors for cluster nucleation and applied them to the NO_3RR (Figure 8a) [88]. The study revealed an asymmetric electron distribution between the Cu atom

adjacent to Sn and the distal Cu atom. The introduction of defective carbon further enhanced this electronic asymmetry, which optimized the adsorption capacity of specific Cu sites toward NO_3^- (Figure 8b). As a result, the synergy among Sn, Cu, and defective graphene promoted H_2O dissociation and facilitated the reduction of key intermediates, ultimately achieving a 99.5% FE for NH_3 production in a neutral electrolyte. This work highlights that electronic asymmetry in catalysts is a crucial factor for enabling efficient multistep catalysis. Xu et al. successfully synthesized Cu nanocluster catalysts embedded within MOFs via an in-situ transformation strategy, using atomically dispersed Cu species in Ce-UiO-66 as the precursor (Figure 8c,d). The resulting catalyst exhibited remarkable performance in the NO_3RR (5 mM NO_3^-), achieving a high NH_3 FE of 85.5% [89]. It was demonstrated that the MOFs not only effectively stabilized the Cu nanoclusters against aggregation but also engaged in synergistic interactions with them, which significantly lowered the reaction energy barrier and thereby promoted efficient NH_3 formation (Figure 8e). This work provides new perspectives and insights into understanding the host-guest interactions between the host framework and metal clusters. Zhang et al. successfully synthesized Cu-Ni bimetallic cluster catalysts confined within silicalite-1 zeolite (Cu-Ni@S-1) using a hydrothermal method, employing a mixture of Cu-based and Ni-based complexes as precursors (Figure 8f) [90]. This catalyst was subsequently applied to the NO_3RR. Research indicated that the confinement effect of silicalite-1 zeolite elevated the d-band centers of the metals, thereby enhancing the catalyst's adsorption capacity for NO_3^-. Furthermore, the incorporation of Cu narrowed the energy gap between the nickel 3d and N 2p orbitals, strengthening the adsorption of the *NOH intermediate (Figure 8g). Therefore, in this catalytic system, the synergy between the bimetallic clusters and the zeolite confinement effect collectively promotes the efficient conversion of NO_3^- to NH_3. While the above studies show that synergistic effects in metal clusters can effectively boost the NH_3 production rate, precisely controlling the atomic number of metal clusters on the support surface remains a central challenge.

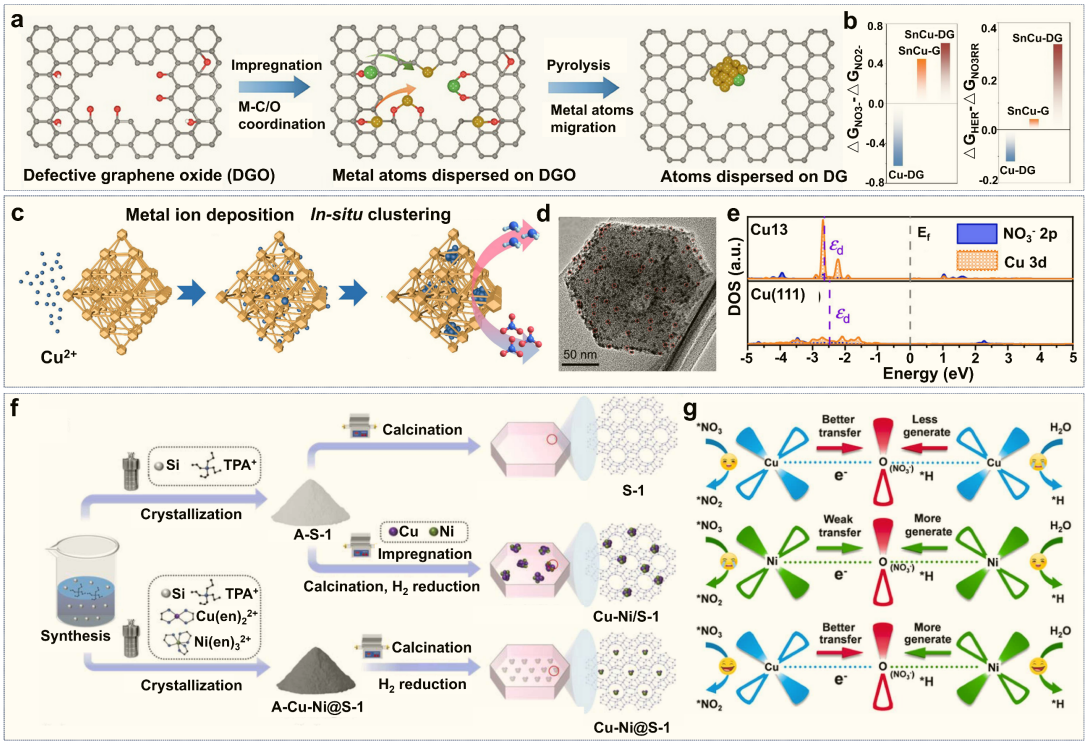

Figure 8. (**a**) The synthesis process of SnCu-DG catalysts, (**b**) the free-energy differences between nitrate and nitrite ions and between the HER and NO_3RR across the three catalysts. Reproduced with permission [88]. Copyright 2025, Wiley. (**c**) The synthesis procedure of the Cu-based cluster catalyst and (**d**) its corresponding TEM image, (**e**) projected density of states of NO_3^- on Cu_{13} and Cu (111). Reproduced with permission [89]. Copyright 2022, American Chemical Society. (**f**) The synthesis process of Cu-Ni@S-1 catalysts and (**g**) the bimetallic synergistic mechanism for NO_3RR. Reproduced with permission [90]. Copyright 2025, Elsevier.

3.4. Metal Nanoparticle Catalysts

NO_3RR on nanoparticle catalysts usually relies on synergistic regulation of multi-metal systems, interfacial effects, crystalline phase structures, and geometric configurations. For instance, by constructing high-entropy alloys (HEAs) catalysts, the electronic synergistic effects between their multiple metallic components can be fully

exploited. Inspired by the structural advantages of high-entropy perovskites, Zhou et al. successfully synthesized the high-entropy perovskite oxide LaB_5O_3, featuring a B-site composed of five metals: Fe, Cu, Co, Cr, and Ni (Figure 9a). This compound was subsequently applied to the NO_3RR (Figure 9b,c) [91]. By integrating crystal phase engineering with a high-entropy strategy, the research achieved a structural transformation from an orthorhombic to a cubic phase. This transformation effectively modulated the spin states of B-site metals, optimized the electronic occupation of iron e_g orbitals, and induced a high-spin configuration with more unpaired electrons than the orthorhombic phase (Figure 9d). As a result, the adsorption of NO_3^- is significantly enhanced, leading to a remarkable FE of 95.83% for the NO_3RR. This work provides novel insights for the rational design of the NO_3RR catalysts, demonstrating an effective strategy for synergistically optimizing catalytic performance through crystalline phase engineering and high-entropy characteristics. Moreover, the synergistic interaction between crystal phases and interfaces can effectively reduce the reaction energy barrier for key intermediates in the NO_3RR. Ma et al. fabricated a 4H/fcc Au-Cu heterostructure with a beaded bracelet configuration via a seed-mediated approach, wherein Cu grew like beads along the Au nanowires (Figure 9e) [92]. By adjusting the surfactant dosage, the coverage density of Cu on the Au nanowires could be modulated, enabling precise control over the exposure density of the Au/Cu interfaces. When applied to the NO_3RR, this catalyst achieved an NH_3 FE of 98.9% with an NH_3 production rate of 116.2 mg h^{-1} cm^{-2} in a flow cell (Figure 9f–h). Mechanistic studies suggested that the Au sites reduced NO_3^- to NO_2^- and NO intermediates, which were then transferred via the Au/Cu interface to the Cu sites for subsequent reduction. Furthermore, compared to the fcc phase, the 4H phase of Cu facilitated more favorable electron transfer. Consequently, this tandem synergistic catalysis involving phase regulation and interface control effectively enhances the catalyst's catalytic activity.

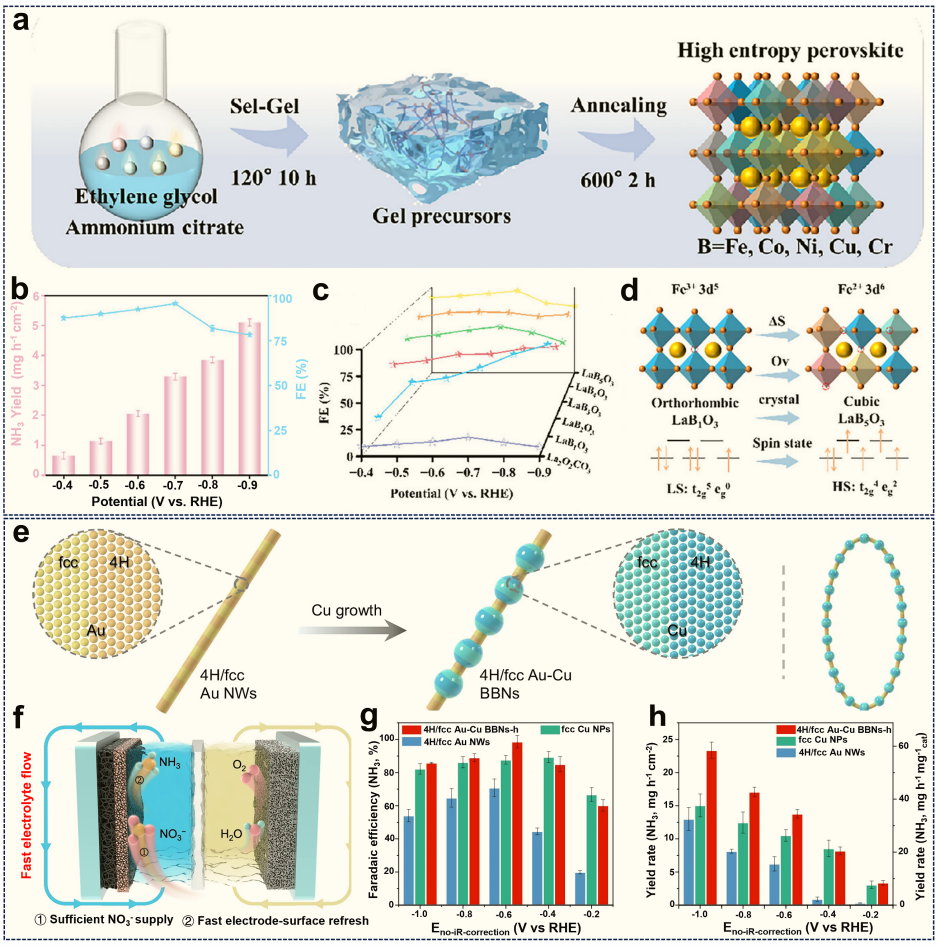

Figure 9. (**a**) The synthesis process of HEA catalysts, (**b**) the catalytic performance of LaB_5O_3, (**c**) comparison of catalysts for NO_3RR, (**d**) schematic diagram of the electronic configuration and spin states of Fe. Reproduced with permission [91]. Copyright 2026, Wiley. (**e**) The synthesis process of 4H/fcc Au-Cu BBNs catalysts, and (**f**) schematic diagram of NO_3RR in a flow reactor. (**g**,**h**) The catalytic performance for NO_3RR. Reproduced with permission [92]. Copyright 2025, Springer Nature.

Although nanoparticle catalysts are easier to fabricate than SACs, DACs, or metal cluster catalysts, their heterogeneous active sites and non-uniform size distribution pose significant challenges in unraveling the precise synergistic mechanisms among different sites [93]. This, in turn, impedes a fundamental understanding of their catalytic nature and constrains the rational design and development of highly efficient catalysts. To facilitate a clear understanding of the distinct catalyst properties, Table 1 summarizes the synergistic strategies, catalytic performance, advantages, and current limitations of each catalyst type discussed in this review.

Table 1. Comparison of synergistic strategies, catalytic performance, advantages, and limitations of different types of catalysts discussed in the text.

Catalyst Types	Catalysts	Synergistic Strategies	FE (%)	NH_3 Yield	Advantages and Limitations	Ref.
SACs	Co-N_4S_1	Interdependency in structure	88.8	9.46 mg h^{-1} mg_{cat}^{-1}	Advantages: high atom utilization and uniform active sites	[72]
	Cu-cis-N_2O_2	Interdependency in structure	80	27.84 mg h^{-1} cm^{-2}		[73]
	Cu_{SA}-NO/C	Interdependency in structure	92.7	24.9 mg h^{1} mg_{Cu}^{-1}	Limitations: low active site density and lack of site diversity	[74]
DACs	PCN-Cu-DAC	Adjacency in space and cooperation in function	100	467 mg h^{-1} mg_{cat}^{-1}	Advantages: tunable electronic/geometric structure and versatile coordination to intermediates	[77]
	RuCu DAs/NGA	Adjacency in space and cooperation in function	95.7	3.1 mg h^{-1} cm^{-2}		[78]
	IPN-CuCo DACs	Adjacency in space and cooperation in function	99	22 mmol h^{-1} cm^{-2}	Limitations: prone to mixed sites and difficult to synthesize precisely	[81]
Metal clusters	$Cu_4(PTI)_4$	Interdependency in structure	100	2.6 mg h^{-1} mg^{-1}	Advantages: multi-metal site synergy and quantum size effect	[85]
	$Cu_4(BTT)_4$	Interdependency in structure	75	1.8 mg h^{-1} mg^{-1}		[85]
	$[Ag_{30}Pd_4(C_6H_9)_{26}](BPh_4)_2$	Interdependency in structure and Cooperation in function	90	2.3 mmol h^{-1} mg^{-1}		[18]
	$Ru_1Au_6(TBBT)PPh_3$	Interdependency in structure and Cooperation in function	95	7 mg mg_{cat}^{-1} h^{-1}		[86]
	Ni_6@CuFe-LDH	Interdependency in structure	97	0.91 mmol mg^{-1} h^{-1}		[87]
	SnCu-DG	Interdependency in structure	99.5	2.61 × 10^{-17} mmol h^{-1} $site_{Cu}^{-1}$	Limitations: high surface free energy leading to agglomeration	[88]
	1-Cu	Interdependency in structure	85.5	66 μmol h^{-1} cm^{-2}		[89]
	Cu-Ni@S-1	Interdependency in structure	-	-		[90]
Metal Nanoparticles	LaB_5O_3	Interdependency in structure	95.8	5 mg h^{-1} cm^{-2}	Advantages: facile synthesis and scalable application.	[91]
	4H/fcc Au-Cu	Interdependency in structure and cooperation in function	98.9	116.2 mg h^{-1} cm^{-2}	Limitations: non-uniform active sites and low atom utilization	[92]

4. Conclusions and Perspectives

Given the severe energy, climate, and environmental issues today, catalytic science is expected to play an indispensable role in modern society. Considering the catalytic processes involving intricate reaction networks and requiring the precise synergy of multiple sites, the design of synergistic catalysts has emerged as a cutting-edge direction within the field of rational catalyst design. Synergistic catalysts integrate multiple functional units within a catalytic system, forming strong correlations through spatial or electronic interactions, thereby exerting complementary effects during the reaction. This not only effectively lowers the reaction energy barriers at key steps and stabilizes specific intermediates but also has the potential to open up new reaction pathways. The NO_3RR

involves complex pathways such as multi-electron transfer and the formation of various intermediates. Therefore, it is necessary to design and utilize synergistic catalysts that leverage electronic and/or structural synergies between different active sites to optimize the reaction pathway and lower the reaction energy barrier, thereby ultimately improving the efficiency and selectivity of ammonia synthesis. In this review, we first emphasized the design principles for synergistic catalysts, elaborating upon them from three perspectives: spatial adjacency, structural interdependence, and functional cooperativity. It is expected to provide useful references for future efforts by extracting common principles of synergistic catalyst design. Subsequently, from the perspective of metal active site scales, focusing on catalysts such as SACs, DACs, clusters, and nanoparticles, the synergistic mechanisms of these catalysts in the NO_3RR were elaborated in detail. In NO_3RR, SACs primarily rely on the synergistic interaction between the metal and the support, or coordination environment. It is noteworthy that by modulating the coordination environment of the single-atom metal to break its coordination symmetry or polarity, the catalytic performance can be effectively optimized. DACs retain the advantages of single-atom sites, while introducing additional active sites enhances the activation ability toward substrates. Metal cluster catalysts involve multiple synergistic mechanisms, including metal-metal, metal-ligand, and cluster-support interactions. The synergy in nanoparticle catalysts typically originates from interactions between different interfaces or components.

Currently, although significant progress has been made in the study of synergistic catalytic strategies for NO_3RR, several key challenges remain to be urgently addressed. To this end, this paper presents the following prospects for the design of synergistic catalysts for NO_3RR.

1. Intermetallic regulation has been applied in atomic-dispersed catalysts, including DACs, alloy clusters, and alloy nanoparticles. Compared to single-component metal, active sites comprising two or more metals offer a broader regulatory space, including aspects such as proportion, site distance, and combination patterns. However, this also introduces significant complexity in achieving uniformity during preparation and precise identification of active sites. Therefore, preparing bimetallic/multi-metallic catalysts with uniform and stable composition and structure, and elucidating their synergistic catalytic mechanisms through in-situ characterization techniques, represent crucial future directions in multi-metallic synergistic catalysis.
2. For supported catalysts, the structural imprecision of the supports makes it challenging to accurately elucidate the synergistic mechanisms involved. Our previously developed Ag_4Pt_2-S-Ti_4 catalyst successfully achieved precise atomic-scale assembly and synergy of bi-clusters, offering a valuable model for constructing well-defined metal-support synergistic systems [75]. Therefore, designing structurally well-defined supports to clarify metal-support synergistic mechanisms in supported catalysts will also emerge as a key research direction for developing highly efficient synergistic catalysts for NO_3RR in the future.
3. Current performance evaluations of synergistic catalysts for the NO_3RR are primarily conducted under laboratory conditions, which are different from real industrial scenarios. To meet the demands of industrial applications, future designs of NO_3RR synergistic catalysts should be evaluated at industrial-level current densities and tested in authentic wastewater environments. The complex composition of real wastewater imposes high requirements on both the catalytic performance and long-term stability of the catalysts.
4. The coupling of nitrate electroreduction with other reactions to produce high-value-added chemicals (e.g., urea, oximes, amino acids) has received widespread attention. The activation of multiple substrates and the more complex electron and proton transfer processes pose new challenges for the understanding of synergistic catalytic mechanisms, calling for a systematic review.
5. Although numerous studies have demonstrated the great potential of well-designed synergistic sites in enhancing catalytic performance, whether these synergistic configurations can remain stable under realistic reaction conditions remains unknown. Future research urgently requires the introduction of operando characterization techniques to track, in real time, the atomic-level structural evolution of synergistic sites during catalytic reactions, thereby clarifying the relationship between “static design” and “dynamic reconstruction”.

Author Contributions

J.L. prepared the original draft and conducted literature curation; H.W. developed the visualizations and performed mechanistic analysis for Figures 1 and 2; Y.M. conducted literature curation; Y.Z. supervised the overall project. All authors have read and agreed to the published version of the manuscript.

Funding

This work was supported by the National Natural Science Foundation of China (92461312, 22125202, U24A20487).

Data Availability Statement

The data generated during this study are available in the main text.

Conflicts of Interest

The authors declare no conflict of interest.

Use of AI and AI-Assisted Technologies

No AI tools were utilized for this paper.

References

1. Kim, U.B.; Jung, D.J.; Jeon, H.J.; et al. Synergistic Dual Transition Metal Catalysis. *Chem. Rev.* **2020**, *120*, 13382–13433.
2. Yang, Q.; Fedorova, E.A.; Cao, D.-B.; et al. Understanding Mn-Modulated Restructuring of Fe-Based Catalysts for Controlling Selectivity in CO_2 Hydrogenation to Olefins. *Nat. Catal.* **2025**, *8*, 595–606.
3. Wang, Y.; Bao, P.; Dong, X.; et al. Thiophenol-Catalyzed Radical Hydroformylation of Unactivated Sterically Hindered Alkenes. *J. Am. Chem. Soc.* **2025**, *147*, 31662–31670.
4. Zhang, B.; Kubis, C.; Franke, R.; Hydroformylation Catalyzed by Unmodified Cobalt Carbonyl under Mild Conditions. *Science* **2022**, *377*, 1223–1227.
5. Ren, X.; Fasan, R. Synergistic Catalysis in an Artificial Enzyme. *Nat. Catal.* **2020**, *3*, 184–185.
6. Ro, I.; Qi, J.; Lee, S.; et al. Bifunctional Hydroformylation on Heterogeneous Rh-WO_x Pair Site Catalysts. *Nature* **2022**, *609*, 287–292.
7. Han, C.; Yang, T.; Fang, Y.; et al. Steering the Product Selectivity of CO_2 Electroreduction by Single Atom Switching in Isostructural Copper Nanocluster Catalysts. *Angew. Chem. Int. Ed.* **2025**, *64*, e202503417.
8. Zhu, J.; Xiao, M.; Ren, D.; et al. Quasi-Covalently Coupled Ni-Cu Atomic Pair for Synergistic Electroreduction of CO_2. *J. Am. Chem. Soc.* **2022**, *144*, 9661–9671.
9. Wang, H.; Cui, G.; Lu, H.; et al. Facilitating the Dry Reforming of Methane with Interfacial Synergistic Catalysis in an Ir@CeO_2 Catalyst. *Nat. Commun.* **2024**, *15*, 3765.
10. Gao, P.; Wang, Q.; Xu, J.; et al. Bronsted/Lewis Acid Synergy in Methanol-to-Aromatics Conversion on Ga-Modified ZSM-5 Zeolites, As Studied by Solid-State NMR Spectroscopy. *ACS Catal.* **2018**, *8*, 69–74.
11. Zhao, M.; Wang, X.; Xu, J.; et al. Strengthening the Metal-Acid Interactions by Using CeO_2 as Regulators of Precisely Placing Pt Species in ZSM-5 for Furfural Hydrogenation. *Adv. Mater.* **2024**, *36*, 2313596.
12. Gordon, C.P.; Engler, H.; Tragl, A.S.; et al. Efficient Epoxidation over Dinuclear Sites in Titanium Silicalite-1. *Nature* **2020**, *586*, 708–713.
13. Jiao, F.; Bai, B.; Li, G.; et al. Disentangling the Activity-Selectivity Trade-Off in Catalytic Conversion of Syngas to Light Olefins. *Science* **2023**, *380*, 727–730.
14. Zhou, Y.; Wei, F.; Qi, H.; et al. Peripheral-Nitrogen Effects on the Ru1 Centre for Highly Efficient Propane Dehydrogenation. *Nat. Catal.* **2022**, *5*, 1145–1156.
15. Gu, Y.; Zhao, E.-D.; Wan, X.; et al. Reaction-Induced Phase Engineering of CuCO Nanoparticles for Enhanced Photothermal CO_2 Hydrogenation. *Adv. Mater.* **2026**, *38*, e15661.
16. Gao, R.; Mao, S.; Lu, B.; et al. Efficient Upcycling of Polyolefin Waste to Light Aromatics via Coupling C-C Scission and Carbonylation. *Angew. Chem. Int. Ed.* **2025**, *64*, e202424334.
17. Han, S.; Li, H.; Li, T.; et al. Ultralow Overpotential Nitrate Reduction to Ammonia Via a Three-Step Relay Mechanism. *Nat. Catal.* **2023**, *6*, 402–414.
18. Qin, L.; Sun, F.; Gong, Z.; et al. Electrochemical NO_3- Reduction Catalyzed by Atomically Precise $Ag_{30}Pd_4$ Bimetallic Nanocluster: Synergistic Catalysis or Tandem Catalysis? *ACS Nano* **2023**, *17*, 12747–12758.
19. Wang, J.; Feng, T.; Chen, J.; et al. Electrocatalytic Nitrate/Nitrite Reduction to Ammonia Synthesis Using Metal Nanocatalysts and Bio-Inspired Metalloenzymes. *Nano Energy* **2021**, *86*, 106088.
20. Zheng, S.-J.; Dong, X.-Y.; Chen, H.; et al. Unveiling Ionized Interfacial Water-Induced Localized H* Enrichment for Electrocatalytic Nitrate Reduction. *Angew. Chem. Int. Ed.* **2025**, *64*, e202413033.
21. Sun, W.; Hu, J.; Shuai, Y.; et al. Beyond Monosite Catalysis: Multi-Tiered Site Engineering for Advanced CO_2 Valorization. *Adv. Funct. Mater.* **2026**, *36*, e22973.
22. Wang, A.; Zhang, L.; Yu, Z.; et al. Ethylene Methoxycarbonylation over Heterogeneous Pt1/MoS_2 Single-Atom Catalyst: Metal-Support Concerted Catalysis. *J. Am. Chem. Soc.* **2024**, *146*, 695–706.
23. Zhao, X.; Wang, F.; Kong, X.-P.; et al. Dual-Metal Hetero-Single-Atoms with Different Coordination for Efficient Synergistic Catalysis. *J. Am. Chem. Soc.* **2021**, *143*, 16068–16077.

24. Yao, S.; Zhang, X.; Zhou, W.; et al. Atomic-Layered Au Clusters on A-Moc as Catalysts for the Low-Temperature Water-Gas Shift Reaction. *Science* **2017**, *357*, 389–393.
25. Huang, X.; Akdim, O.; Douthwaite, M.; et al. Au-Pd Separation Enhances Bimetallic Catalysis of Alcohol Oxidation. *Nature* **2022**, *603*, 271–275.
26. Kattel, S.; Ramírez, P.J.; Chen, J.G.; et al. Active Sites for CO_2 Hydrogenation to Methanol on Cu/ZnO Catalysts. *Science* **2017**, *355*, 1296–1299.
27. Luo, Y.; Wang, X.; Gao, F.; et al. From Single Atom Photocatalysts to Synergistic Photocatalysts: Design Principles and Applications. *Adv. Funct. Mater.* **2025**, *35*, 2418427.
28. Teng, X.; Si, D.; Chen, L.; et al. Synergetic Catalytic Effects by Strong Metal-Support Interaction for Efficient Electrocatalysis. *eScience* **2024**, *4*, 100272.
29. Wu, C.H.; Liu, C.; Su, D.; et al. Bimetallic Synergy in Cobalt-Palladium Nanocatalysts for CO Oxidation. *Nat. Catal.* **2019**, *2*, 78–85.
30. Wang, X.; Lin, Y.; Chen, Y.; et al. Electrospinning High-Entropy Oxide Nanofibers for Catalytic Oxidation of Ethyl Acetate: Unraveling the synergistic role of Metal-Oxygen Bonds. *Sci. China Mater.* **2025**, *68*, 1867–1879.
31. Yang, Q.; Xu, Q.; Jiang, H.-L. Metal-Organic Frameworks Meet Metal Nanoparticles: Synergistic Effect for Enhanced Catalysis. *Chem. Soc. Rev.* **2017**, *46*, 4774–4808.
32. Zhang, X.; Zhou, Q.; Li, C.; et al. Thermodynamic and Kinetic Modulation of Artificial H_2O_2 Photosynthesis via Spatial Control of Redox Catalytic Sites. *J. Am. Chem. Soc.* **2026**, *148*, 11068–11080.
33. Hosseini, M.; Barakat, T.; Cousin, R.; et al. Catalytic Performance of Core-Shell and alloy Pd-Au Nanoparticles for total oxidation of VOC: The effect of Metal Deposition. *Appl. Catal. B Environ.* **2012**, *111–112*, 218–224.
34. Xu, M.; Yao, S.; Rao, D.; et al. Insights into Interfacial Synergistic Catalysis over Ni@TiO_2-x Catalyst toward Water-Gas Shift Reaction. *J. Am. Chem. Soc.* **2018**, *140*, 11241–11251.
35. Xu, D.; Zhang, S.-N.; Chen, J.-S.; et al. Design of the Synergistic Rectifying Interfaces in Mott-Schottky Catalysts. *Chem. Rev.* **2023**, *123*, 1–30. https://doi.org/10.1021/acs.chemrev.2c00426.
36. Jiang, Z.; Sun, W.; Shang, H.; et al. Atomic Interface Effect of a Single Atom Copper Catalyst for Enhanced Oxygen Reduction Reactions. *Energy Environ. Sci.* **2019**, *12*, 3508–3514.
37. Pan, Y.; Zhang, C.; Liu, Z.; et al. Structural Regulation with Atomic-Level Precision: From Single-Atomic Site to Diatomic and Atomic Interface Catalysis. *Matter* **2020**, *2*, 78–110.
38. An, Q.; Bo, S.; Jiang, J.; et al. Atomic-Level Interface Engineering for Boosting Oxygen Electrocatalysis Performance of Single-Atom Catalysts: From Metal Active Center to the First Coordination Sphere. *Adv. Sci.* **2023**, *10*, 2205031.
39. Geng, S.; Ren, R.; Qin, R.; et al. Lattice Mismatched Platinum-Tellurium@Platinum-Ruthenium Core@Shell Nanorods Achieve Ultrahigh Alkaline Hydrogen Electrocatalysis for Dual Practical Devices. *Adv. Mater.* **2025**, *37*, e17683.
40. Zhang, X.; Sun, Z.; Jin, R.; et al. Conjugated Dual Size Effect of Core-Shell Particles Synergizes Bimetallic Catalysis. *Nat. Commun.* **2023**, *14*, 530.
41. Wang, A.-L.; Xu, H.; Feng, J.-X.; et al. Design of Pd/PANI/Pd Sandwich-Structured Nanotube Array Catalysts with Special Shape Effects and Synergistic Effects for Ethanol Electrooxidation. *J. Am. Chem. Soc.* **2013**, *135*, 10703–10709.
42. Wang, Z.; Yi, Z.; Wong, L.W.; et al. Oxygen Doping Cooperated with Co-N-Fe Dual-Catalytic Sites: Synergistic Mechanism for Catalytic Water Purification within Nanoconfined Membrane. *Adv. Mater.* **2024**, *36*, 2404278.
43. Wang, H.; Luo, W.; Zhu, L.; et al. Synergistically Enhanced Oxygen Reduction Electrocatalysis by Subsurface Atoms in Ternary PdCuNi Alloy Catalysts. *Adv. Funct. Mater.* **2018**, *28*, 1707219.
44. Jin, Z.; Li, P.; Meng, Y.; et al. Understanding the inter-site distance effect in Single-Atom Catalysts for Oxygen Electroreduction. *Nat. Catal.* **2021**, *4*, 615–622.
45. Gao, M.; Tian, F.; Guo, Z.; et al. Mutual-Modification Effect in Adjacent Pt Nanoparticles and Single Atoms with Sub-Nanometer Inter-Site Distances to Boost Photocatalytic Hydrogen Evolution. *Chem. Eng. J.* **2022**, *446*, 137127.
46. Sun, W.; Tang, Y.; Dong, H.; et al. Inter-Site Distance Engineering of Heteronuclear Pd-Cu Atomic Sites Enables High-Efficiency Cross-Coupling Reactions through Atomic-Scale Locking Pockets. *Adv. Funct. Mater.* **2025**, *35*, e08858.
47. Xiang, J.; Wang, P.; Li, P.; et al. Inter-Site Distance Effect in Electrocatalysis. *Angew. Chem. Int. Ed.* **2025**, *64*, e202500644.
48. Wang, T.; Hu, J.; Ouyang, R.; et al. Nature of metal-support interaction for Metal Catalysts on Oxide Supports. *Science* **2024**, *386*, 915–920.
49. Luo, Z.; Zhao, G.; Pan, H.; et al. Strong Metal-Support Interaction in Heterogeneous Catalysts. *Adv. Energy Mater.* **2022**, *12*, 2201395.
50. Hu, S.; Li, W.-X.; Sabatier Principle of Metal-Support Interaction for Design of Ultrastable Metal Nanocatalysts. *Science* **2021**, *374*, 1360–1365.
51. van Deelen, T.W.; Hernández Mejía, C.; de Jong, K.P.; Control of Metal-Support Interactions in Heterogeneous Catalysts to Enhance Activity and Selectivity. *Nat. Catal.* **2019**, *2*, 955–970.

52. Wu, X.; Wang, C.; Huang, Y.; et al. Synergistic Effect of Curvature and Coordination Environment on the Catalytic Performance of Single-Atom Catalysts for Nitrogen Reduction Reaction. *Appl. Surf. Sci.* **2026**, *725*, 165734.
53. Liu, Y.; Yang, N.; Feng, H.; et al. Engineering Heterogeneous Dual-Coordination Environments for Single-Atom Nickel Catalysts: A Synergistic Strategy to Enhance Selective Hydrogenation. *J. Am. Chem. Soc.* **2025**, *147*, 45966–45976.
54. Zhang, L.; Yang, X.; Lin, J.; et al. On the Coordination Environment of Single-Atom Catalysts. *Acc. Chem. Res.* **2025**, *58*, 1878–1892.
55. Hannagan, R.T.; Giannakakis, G.; Flytzani-Stephanopoulos, M. Single-Atom Alloy Catalysis. *Chem. Rev.* **2020**, *120*, 12044–12088.
56. Liu, Z.; Tan, H.; Li, B.; et al. Ligand Effect on Switching the Rate-Determining Step of Water Oxidation in Atomically Precise Metal Nanoclusters. *Nat. Commun.* **2023**, *14*, 3374.
57. Cai, X.; Wang, H.; Tian, Y.; et al. Catalytic Application of Atomically Precise Metal Clusters in Selective Hydrogenation Processes. *ACS Catal.* **2024**, *14*, 11918–11930.
58. Sun, H.; Yang, J.; Sun, M.; et al. Lewis Acid-Mediated Interface Engineering for Enhanced Electrocatalytic Energy Conversion. *Adv. Funct. Mater.* **2025**, *35*, e19393.
59. Bailleul, S.; Yarulina, I.; Hoffman, A.E.J.; et al. A Supramolecular View on the Cooperative Role of Brønsted and Lewis Acid Sites in Zeolites for Methanol Conversion. *J. Am. Chem. Soc.* **2019**, *141*, 14823–14842.
60. Peng, S.-S.; Shao, X.-B.; Gu, M.-X.; et al. Catalytically Stable Potassium Single-Atom Solid Superbases. *Angew. Chem. Int. Ed.* **2022**, *61*, e202215157.
61. Grimaud, A.; Diaz-Morales, O.; Han, B.; et al. Activating Lattice Oxygen Redox Reactions in Metal Oxides to Catalyse Oxygen Evolution. *Nat. Chem.* **2017**, *9*, 457–465.
62. Shi, R.; Zhao, Y.; Waterhouse, G.I.N.; et al. Defect Engineering in Photocatalytic Nitrogen Fixation. *ACS Catal.* **2019**, *9*, 9739–9750.
63. Huang, Y.-B.; Liang, J.; Wang, X.-S.; et al. Multifunctional Metal-Organic Framework Catalysts: Synergistic Catalysis and Tandem Reactions. *Chem. Soc. Rev.* **2017**, *46*, 126–157.
64. Yuan, P.; Wun, C.K.T.; Lo, T.W.B. Harnessing Synergistic Cooperation of Neighboring Active Motifs in Heterogeneous Catalysts for Enhanced Catalytic Performance. *Adv. Mater.* **2025**, *37*, 2501960.
65. Sandoval-Diaz, L.; Cruz, D.; Vuijk, M.; et al. Metastable Nickel-Oxygen Species Modulate Rate Oscillations During Dry Reforming of Methane. *Nat. Catal.* **2024**, *7*, 161–171.
66. Shen, D.; Li, Z.; Shan, J.; et al. Synergistic Pt-CeO_2 Interface Boosting Low Temperature Dry Reforming of Methane. *Appl. Catal. B Environ. Energy* **2022**, *318*, 121809.
67. Buelens, L.C.; Galvita, V.V.; Poelman, H.; et al. Super-Dry Reforming of Methane Intensifies CO_2 Utilization via Le Chatelier's Principle. *Science* **2016**, *354*, 449–452.
68. Zhu, Q.; Zhou, H.; Wang, L.; et al. Enhanced CO_2 Utilization in Dry Reforming of Methane Achieved through Nickel-Mediated Hydrogen Spillover in Zeolite Crystals. *Nat. Catal.* **2022**, *5*, 1030–1037.
69. Tang, Y.; Wang, H.; Guo, C.; et al. Synergies Between Atomically Dispersed Ru Single Atoms and Nanoparticles on $CeAlO_x$ for Enhanced Photo-Thermal Catalytic CO_2 Hydrogenation. *Adv. Mater.* **2026**, *38*, e12793.
70. Zhang, X.; Yan, T.; Hou, H.; et al. Regioselective Hydroformylation of Propene Catalysed by Rhodium-Zeolite. *Nature* **2024**, *629*, 597–602.
71. Liang, X.; Yao, S.; Li, Z.; et al. Challenge and Chance of Single Atom Catalysis: The Development and Application of the Single Atom Site Catalysts Toolbox. *Acc. Chem. Res.* **2025**, *58*, 1607–1619.
72. Wei, J.; Wang, Q.; Song, X.; et al. Anisotropic Etching Induced Construction of Co-N4S1 Single-Atom Sites on 2D Hierarchical Porous Honeycomb Carbon with Enhanced Mass Transfer for Efficient Electrocatalysis. *Adv. Funct. Mater.* **2025**, *35*, e07281.
73. Cheng, X.-F.; He, J.-H.; Ji, H.-Q.; et al. Coordination Symmetry Breaking of Single-Atom Catalysts for Robust and Efficient Nitrate Electroreduction to Ammonia. *Adv. Mater.* **2022**, *34*, 2205767.
74. Li, Y.; Guo, J.; Yang, Y.; et al. Atomically Dispersed Copper Electrocatalysts with Proton-feeding Centers for Efficient Ammonia Synthesis by Nitrate Electroreduction. *Adv. Funct. Mater.* **2026**, *36*, e08619.
75. Song, T.; Shen, C.; Tian, Y.; et al. A Heterodimeric Cluster-Based Pair Catalyst for Electrochemical Synthesis of Cyclohexanone Oxime. *Angew. Chem. Int. Ed.* **2025**, *64*, e202507569.
76. Lu, J.; Mou, Y.; Zhu, Y. Atomically Precise Metal Clusters for Efficient Catalytic Conversion of Nitrate to High-Valued Chemicals. *Chem. Methods* **2026**, *6*, e202500114.
77. Li, Q.; Li, Y.; Xu, B.; et al. Gram-Scale Ammonia Synthesis via Electrochemical Nitrate Reduction Using Enzyme-Inspired Dual-Atomic Cu Catalyst. *Angew. Chem. Inter. Ed.* **2025**, *64*, e202510139.
78. Liu, K.; Sun, Z.; Peng, X.; et al. Tailoring asymmetric RuCu dual-atom electrocatalyst toward ammonia synthesis from nitrate. *Nat. Commun.* **2025**, *16*, 2167.

79. He, W.; Chandra, S.; Quast, T.; et al. Enhanced Nitrate-to-Ammonia Efficiency over Linear Assemblies of Copper-Cobalt Nanophases Stabilized by Redox Polymers. *Adv. Mater.* **2023**, *35*, 2303050.
80. Bu, Y.; Wang, C.; Zhang, W.; et al. Electrical Pulse-Driven Periodic Self-Repair of Cu-Ni Tandem Catalyst for Efficient Ammonia Synthesis from Nitrate. *Angew. Chem. Int. Ed.* **2023**, *62*, e202217337.
81. Su, X.; Li, M.; Wen, Y.; et al. Atomically Paired Cu-Co Dual Sites for Near-Unity Ammonia Selectivity in Nitrate Electroreduction. *J. Am. Chem. Soc.* **2025**, *147*, 46471–46482.
82. Jang, W.; Oh, D.; Lee, J.; et al. Homogeneously Mixed Cu-Co Bimetallic Catalyst Derived from Hydroxy Double Salt for Industrial-Level High-Rate Nitrate-to-Ammonia Electrosynthesis. *J. Am. Chem. Soc.* **2024**, *146*, 27417–27428.
83. Song, T.; Liu, X.; Wang, H.; et al. Catalytic conversion of Carbon Dioxide Over Atomically Precise Metal Clusters Toward Fine Chemicals. *Coord. Chem. Rev.* **2025**, *543*, 216922.
84. Jin, R.; Li, G.; Sharma, S.; et al. Toward Active-Site Tailoring in Heterogeneous Catalysis by Atomically Precise Metal Nanoclusters with Crystallographic Structures. *Chem. Rev.* **2021**, *121*, 567–648.
85. Chen, H.; Qi, K.-S.; Dong, X.-Y.; et al. Ligand-Mediated Activity of Cu_4 Clusters Boosts Electrocatalytic Nitrate Reduction. *Angew. Chem. Int. Ed.* **2025**, *64*, e20251042.
86. Lu, J.; Shen, C.; Tian, Y.; et al. An Atomically Precise $Ru_1Au_6(TBBT)_6(PPh_3)_6$ Cluster Catalyst for Ammonia Production. *Angew. Chem. Int. Ed.* **2025**, *64*, e202516398.
87. Gu, X.; Zhang, J.; Guo, S.; et al. Tiara Ni Clusters for Electrocatalytic Nitrate Reduction to Ammonia with 97% Faradaic Efficiency. *J. Am. Chem. Soc.* **2025**, *147*, 22785–22795.
88. Wu, Q.; Han, Y.; Wu, L.; et al. Constructing Asymmetric Sn-Cu-C Interface via Defective Carbon Trapped Atomic Clusters for Efficient Neutral Nitrate Reduction. *Adv. Mater.* **2025**, *37*, 2505743.
89. Xu, Y.-T.; Xie, M.-Y.; Zhong, H.; et al. *In Situ* Clustering of Single-Atom Copper Precatalysts in a Metal-Organic Framework for Efficient Electrocatalytic Nitrate-to-Ammonia Reduction. *ACS Catal.* **2022**, *12*, 8698–8706.
90. Zhang, J.; Liu, L.; Hu, N.; et al. Accelerating Proton Coupled Electron Transfer by Confined Cu-Ni Bimetallic Clusters for Boosting Electrochemical Hydrodeoxygenation of Nitrate. *Appl. Catal. B Environ. Energy* **2025**, *371*, 125195.
91. Zhou, L.; Feng, D.; Li, Z.; et al. High-Spin-State Engineering in High-Entropy Perovskite Oxides via Crystal Phase Modulation for Paired Electrochemical Nitrate Reduction and Sulfur Ion Oxidation. *Adv. Funct. Mater.* **2025**, *35*, e14375.
92. Ma, Y.; Guo, L.; Chang, L.; et al. Unconventional Phase Metal Heteronanostructures with Tunable Exposed Interface for Efficient Tandem Nitrate Electroreduction to Ammonia. *Nat. Commun.* **2025**, *16*, 7632.
93. Li, Z.; Ji, S.; Liu, Y.; et al. Well-Defined Materials for Heterogeneous Catalysis: From Nanoparticles to Isolated Single-Atom Sites. *Chem. Rev.* **2020**, *120*, 623–682.